RSC Advances

PAPER

View Article Online
View Journal | View Issue

Cite this: RSC Adv., 2018, 8, 39115

Solution-processed amorphous ZrO_2 gate dielectric films synthesized by a non-hydrolytic sol–gel route†

Jong-Baek Seon,[a] Nam-Kwang Cho,[a] Gayeong Yoo,[a] Youn Sang Kim*[ab] and Kookheon Char*[c]

Received 18th August 2018
Accepted 7th November 2018

DOI: 10.1039/c8ra06911e

rsc.li/rsc-advances

Solution-processed zirconium oxide (ZrO_2) dielectrics were formed *via* a non-hydrolytic sol–gel route at low-temperature, and are suitable for flexible thin film transistor (TFT) devices. Precursor solutions with equimolar zirconium halide and zirconium alkoxide were prepared, and amorphous ZrO_2 films were obtained by spin-coating and annealing at 300 °C through the direct condensation reaction between them. The ZrO_2 films exhibited a high dielectric constant near 10, and a low leakage current density of 5×10^{-8} A cm^{-2} at a field of 1 MV cm^{-1}. High mobility p-type pentacene TFTs were fabricated using the ZrO_2 dielectrics, with a saturation field-effect mobility of 3.7 cm^2 V^{-1} s^{-1}, a threshold voltage of −2.7 V, an on/off ratio of 1.1×10^6 and a subthreshold swing of 0.65 V dec^{-1}.

High dielectric constant (high-*k*) materials have received great interest as alternatives to conventional dielectric materials such as silicon dioxide (SiO_2). These high-*k* dielectrics can be used as key components of the semiconductor and display industry in the form of capacitor dielectrics and transistor gate insulators.[1] In the semiconductor industry, as the traditional gate dielectric becomes extremely thin (∼a few atomic layer thick), leakage currents are generated due to direct tunneling of electrons through the dielectric itself, resulting in power dissipation and heat emission, which is a serious problem to be solved. High-*k* dielectrics are expected to reduce the leakage currents since thicker dielectric layers can be used without altering the required dielectric properties.[1,2] In the display industry, high-*k* dielectrics are considered core materials that allow high on-currents in low voltage operation resulting in low-power consumption devices. Among many high-*k* materials, zirconium oxide (ZrO_2) was chosen because of its outstanding physical and chemical properties such as high intrinsic dielectric constants, high melting points, and great chemical stability.[3] ZrO_2 is an important metal oxide and has been applied to several technologies including gate dielectrics.[2–4]

Compared with vacuum-based processes such as chemical vapor deposition (CVD) and sputtering, solution-based processes (especially sol–gel methods) have distinguished advantages: low-cost and ease of large area deposition. However, solution-processes based on conventional hydrolytic sol–gel methods involve hydrolysis and condensation reactions, which require high thermal energy to form three-dimensional solid networks of pure components.[5] In the past, several groups have reported on the synthesis of inorganic oxides *via* non-hydrolytic sol–gel routes.[6–12] The basis of these methods is the reaction between a metal halide and an oxygen donor in the absence of water. The oxygen donor may be an alkoxide, an ether or an alcohol. The reaction formulae using an alkoxide or an ether as an oxygen donor are as follows.[8–12]

$$MX_n + M(OR)_n \rightarrow 2MO_{n/2} + nRX \text{ (alkoxide route)} \quad (1)$$

$$MX_n + (n/2)ROR \rightarrow MO_{n/2} + nRX \text{ (ether route)} \quad (2)$$

In the above reaction scheme, the ether route is finally followed by the alkoxide route, in which the alkoxide generation is preceded by a substitution reaction between an alkoxide and an ether.

$$\equiv M{-}X + R{-}O{-}R \rightarrow \equiv M{-}OR + R{-}X \quad (3)$$

Finally, the metal oxide network formation is completed through the condensation reaction between the metal halide and the alkoxide as described in eqn (1).

By direct condensation without any hydroxylation of the conventional hydrolytic sol–gel route, the above reactions complete at lower temperatures than the hydrolytic ones.[12] The

---

[a] Program in Nano Science and Technology, Graduate School of Convergence Science and Technology, Seoul National University, Seoul 08826, Republic of Korea. E-mail: younskim@snu.ac.kr

[b] Advanced Institutes of Convergence Technology, 864-1 Iui-dong, Yeongtong-gu, Suwon-si, Gyeonggi-do 16229, Republic of Korea

[c] School of Chemical & Biological Engineering, Seoul National University, Seoul 08826, Republic of Korea. E-mail: khchar@snu.ac.kr

† Electronic supplementary information (ESI) available. See DOI: 10.1039/c8ra06911e

advantages of low temperature process are variously known, including flexible and low-cost processes. The most important characteristic we thought of is the ability to form amorphous films. Amorphous gate insulators are generally preferred because of their smooth surfaces, which eliminates some of problems associated with grain boundaries in crystalline films. The crystalline rough surfaces induce charge trapping and leakage currents, deteriorating the channel mobility and the reliability of thin film devices.[13–16] Even though ZrO_2 crystallizes at much lower temperatures than SiO_2,[2] the crystallinity of thin ZrO_2 films can be controlled by adjusting the process temperature of the non-hydrolytic sol–gel method.

In this letter, we present the solution-processed amorphous ZrO_2 thin films by a non-hydrolytic sol–gel route that can be applied as gate insulators for TFTs. To demonstrate advantages of the high dielectric quality of the ZrO_2 films, we selected a pentacene as channel material for TFT devices. Pentacene was thermally evaporated, which minimizes secondary effects that may influence the properties of the gate insulator, either chemically or thermally. To grow the ZrO_2 thin films, the precursor solution was spin-coated onto Si wafers and glass substrates and then annealed at low temperature (~300 °C). Also, to investigate the physical properties of the thin ZrO_2 films including morphological and electrical characteristics, we carried out several analyses, such as X-ray diffraction (XRD), scanning electron microscopy (SEM), current–voltage (*IV*) and TFT characterization. The ZrO_2 films exhibited a high dielectric constant near 10 and p-type pentacene TFTs with high mobility were fabricated using the ZrO_2 dielectrics, with a saturation field-effect mobility of $3.7\ cm^2\ V^{-1}\ s^{-1}$.

Materials such as zirconium(IV) isopropoxide isopropanol complex ($Zr[OCH(CH_3)_2]_4(CH_3)_2CHOH$), zirconium(IV) chloride ($ZrCl_4$) and 2-methoxy ethanol were used as received without further purification. We prepared equimolar amounts of $ZrCl_4$ and $Zr[OCH(CH_3)_2]_4(CH_3)_2CHOH$ precursor solutions with concentrations of 5 wt% and 16 wt% in 2-methoxyethanol respectively. The prepared solutions were then spin-coated onto silicon and glass substrates at 500 rpm. Finally, the coated substrates were baked at 100 °C on a hot plate for 1 min for solvent evaporation and then post-annealed at 300 °C and 400 °C on a hot plate and 600 °C in a furnace for 1 h for the curing of the thin films to confirm their morphology at each temperature.

To study the electrical properties of the ZrO_2 thin films, we fabricated metal–insulator–metal (MIM) structures (Fig. 1(a)). The dielectric constants, the leakage currents, and the breakdown voltages of the ZrO_2 thin films were measured. TFT devices were also fabricated as shown in Fig. 1(b) to investigate the high-*k* effect of ZrO_2 gate dielectrics with pentacene channel layers. Pentacene channel layers were deposited by thermal evaporation. In both devices, we used shadow masks for patterning aluminum (Al) top electrodes, pentacene channel layer, and gold (Au) source/drain electrodes. In the TFT device structure, molybdenum/tungsten alloy (MoW) gate electrodes were patterned by photolithographic processes.

The thickness of ZrO_2 thin films were measured with a spectroscopic ellipsometer (M-2000V, J. A. Woollam. Co. Inc.).

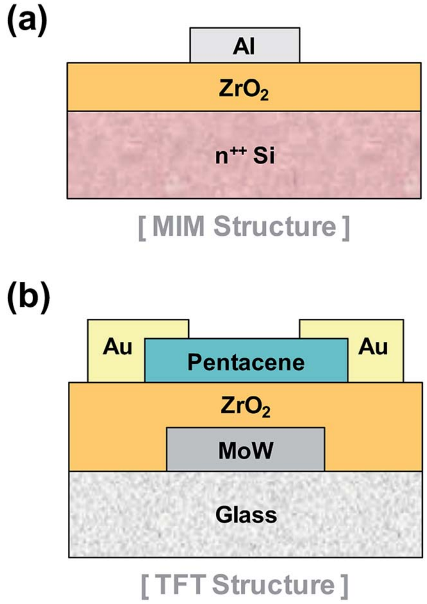

Fig. 1 (a) Metal–insulator–metal (MIM) structure used to measure the dielectric constants, the leakage currents, and the breakdown voltages of the ZrO_2 films (Al diameter = 1 mm). (b) TFT structure with a 700 Å pentacene channel and a 1500 Å ZrO_2 gate dielectric layer (*L* (channel length) = 160 μm; *W* (channel width) = 1 mm).

The film crystallinity was measured at 40 kV and 30 mA using a Phillips X'pert Pro X-ray diffractometer equipped with a Cu Kα source. The surface morphology were measured using a Hitachi S4800 scanning electron microscopy. The dielectric constants of ZrO_2 thin films were measured using an Agilent 4284A precision LCR meter in the frequency range between 20 Hz and 100 kHz. Leakage currents, breakdown voltages and TFT characteristics were measured by a Keithley 4200, semiconductor characterization system.

Through the spin-coating and annealing process, we have obtained thin ZrO_2 films by the non-hydrolytic sol–gel route. The film thicknesses were 420 Å and 1500 Å with concentration of 5 wt% and 16 wt%, respectively. We chose the alkoxide route mentioned in reaction (1), where zirconium chloride and zirconium isopropoxide act as a metal halide and a metal alkoxide (an oxygen donor), respectively. XRD and SEM analyses were performed to confirm the possibility of controlling the film morphology by varying the annealing temperature. Fig. 2 shows the X-ray diffraction patterns of the thin ZrO_2 films with post-annealing temperatures of 300 °C, 400 °C, and 600 °C. An amorphous phase is observed for the samples with 300 °C and 400 °C. Only the sample annealed at 600 °C exhibits a crystalline structure. ZrO_2 exists in three major crystal phases: cubic, tetragonal, and monoclinic polymorphs.[17] In our experiment, the thin films annealed at 600 °C showed the tetragonal phase. From the full width at half maximum height of the peak, the crystalline domain size can be estimated by the Scherrer relation ($L_s = n\lambda/\beta\cos\theta$, where n is unity, λ the wavelength of incident X-rays and θ the diffracted angle). The crystalline domain size was calculated to be about 160 Å, which means that grain boundaries are caused by the nanocrystals in the

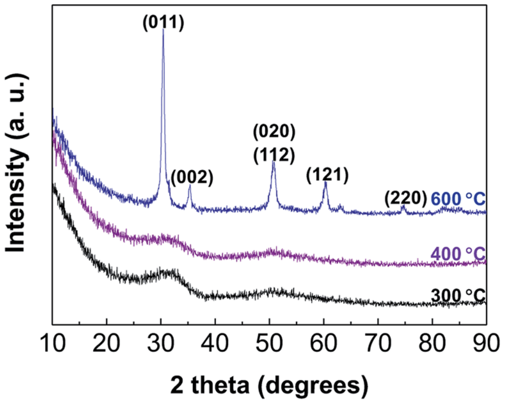

Fig. 2 XRD patterns of the spin-coated thin ZrO_2 films post-annealed at 300 °C, 400 °C, and 600 °C, respectively.

amorphous matrix. Through SEM analysis (Fig. S1†), the morphology of the thin film surface could be confirmed intuitively, and a comprehensive conclusion could be made comparing with the crystallographic analysis of XRD. As expected, the conditions of 300 °C and 400 °C show microscopically flat surfaces, and at 600 °C, it is a rough surface due to the crystal growth as confirmed by XRD. To avoid deleterious effects of the grain boundaries and take advantage of the various features of the low temperature processes, we adopted the low temperature processed (~300 °C) films as gate insulators for TFTs fabrication. In addition, because of the tendency of binary oxides to crystallize at low thermal energy, multi-metal oxides are commonly used to induce amorphous structures.[13] One of the important facts to consider in this work is that reliable amorphous gate insulators can be obtained using only binary oxides at relatively low temperatures by virtue of the non-hydrolytic sol–gel route.

In order to investigate the potential of thin ZrO_2 films as gate insulators of TFTs, the dielectric constants, the leakage currents, and the breakdown voltages of the ZrO_2 thin films were measured. Fig. 3(a) shows the measured dielectric constants of a ZrO_2 film over the predetermined frequency range, indicating a high dielectric constant of about 10 at 100 kHz. This value is generally less than the known value, over 20.[2–4] Our solution-processed thin ZrO_2 films are amorphous and inevitably contain pores as a consequence of the sol–gel process.[5] This, in turn, produces a film of lower density than a vacuum-deposited crystalline film, and as a result the dielectric constant of the film must be small. Even though the non-hydrolytic sol–gel ZrO_2 films have relatively small dielectric constants compared to their vacuum deposited counterparts, the amorphous nature could offset this negative effect by minimizing the grain boundary-induced device instability, and they still have a much higher dielectric constant value than silicon dioxide (~3.9). Fig. 3(b) shows the leakage current characteristics of the ZrO_2 films. The leakage current at an electric field of 1 MV cm^{-1} is observed at about 5×10^{-8} A cm^{-2} and the breakdown voltage is greater than 4 MV cm^{-1}, which demonstrates the applicability of gate dielectrics. Besides, the completion of the ZrO_2 non-hydrolytic sol–gel reaction at a temperature of 300 °C or higher can also be confirmed by the electrical characteristics at 300 °C. Similar dielectric constants were measured according to frequencies. Generally, when the reaction is insufficient, abnormal dielectric constant values appear at high frequencies due to the mobile charges in the films. In addition, low leakage currents also represent a stable ZrO_2 thin film state.

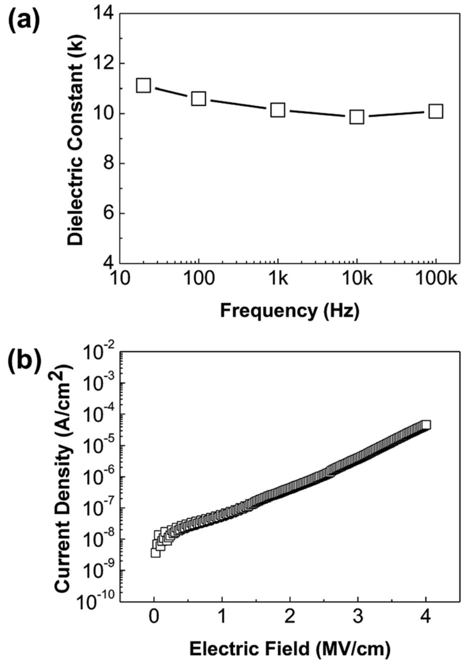

Fig. 3 (a) Dielectric constants of a thin ZrO_2 films as a function of frequency, (b) leakage current across a thin ZrO_2 film.

For the pentacene TFT, a representative output curve of the drain current (I_{DS}) *versus* the drain voltage (V_{DS}) at various gate voltages (V_{GS}) is shown in Fig. 4(a). The TFT demonstrates a typical transistor behaviour. Current saturation is observed at high V_{DS} as the accumulation layer of the pentacene channel is pinched off near the drain electrode. A transfer curve of I_{DS} *versus* V_{GS} with a V_{DS} of −10 V is plotted in Fig. 4(b). By taking the square root of both sides in the following equation, TFT characteristics including the field effect mobility (μ) were obtained in the saturation regime.[18]

$$I_{DS} = \frac{WC_i\mu}{2L}(V_{GS} - V_T)^2 \qquad (4)$$

where, C_i is the areal capacitance of the ZrO_2 insulator, W is the channel width, L is the channel length, V_T is the threshold voltage. The TFTs exhibit excellent device characteristics: a field-effect mobility (μ_{sat}) of 3.7 $cm^2V^{-1}s^{-1}$, a threshold voltage of −2.7 V, a on/off ratio of 1.1×10^6, and a subthreshold swing of 0.65 V dec^{-1}. The field-effect mobility of 3.7 cm^2 V^{-1} s^{-1} at low V_{GS} is one of the highest results reported so far. Compared with pentacene TFTs with SiO_2 gate insulators, the superiority of ZrO_2 high-*k* dielectrics of this study can be demonstrated. In general, for pentacene TFTs with SiO_2 gate insulators, the field effect mobility is less than 1 cm^2 V^{-1} s^{-1},

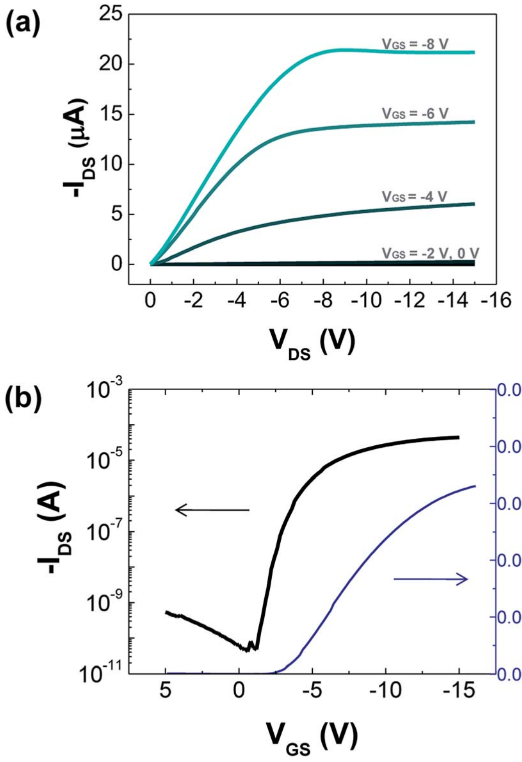

Fig. 4 Device characteristics of spin-coated ZrO_2/pentacene TFT devices. (a) Output characteristics: V_{GS} varied from 0 V to −8 V, (b) Transfer characteristics: $V_{DS} = -10$ V.

which is compared with the mobility of 3.7 $cm^2\ V^{-1}\ s^{-1}$ of this study.[19] This excellent result is attributed to the high-*k* effect and smooth amorphous morphology of the ZrO_2 film. High-*k* dielectrics can induce more charge carriers in the semiconductor channel region. Unlike the traditional metal-oxide-semiconductor field-effect transistor (MOSFET) theory,[20] several studies have shown that mobility depends on *N* (accumulated carriers in the channel) in organic TFTs and support high mobility effect of our experiments.[21–24] This claim is based on the multiple trapping and release (MTR) model, which is widely used for the amorphous silicon (a-Si : H) TFT modeling.[22–24] Lee *et al.* have demonstrated the same relevance for oxide semiconductor TFTs using the MTR model and noted generalization for disordered semiconductor TFTs including the organic TFTs.[25] They modelled the relationship between mobility and capacitance and presented a generalized equation.[25] Another remarkable feature of our results is a very small subthreshold swing. It determines the voltage swing required to switch the device from the "off" to "on" state. The small subthreshold swing allows TFTs with low operating voltage to be implemented.

Conclusions

In summary, we have demonstrated the potential of solution-processed amorphous ZrO_2 high-*k* dielectric films fabricated with a non-hydrolytic sol–gel route at low temperature to realize high-performance devices at low voltage. We have succeeded in fabricating spin-coated ZrO_2 thin films using a non-hydrolytic sol–gel route and demonstrated through chemical reactions that this is possible and have opened up a new way to develop high-*k* dielectrics at low process temperatures (∼300 °C). In spite of amorphous ZrO_2, a dielectric constant near 10 and a low leakage current density of 5×10^{-8} A cm^{-2} at a field of 1 MV cm^{-1} were obtained. Besides, TFTs with these ZrO_2 gate dielectrics showed excellent transistor characteristics: the field-effect mobility at the saturation region of 3.7 $cm^2\ V^{-1}\ s^{-1}$ and the subthreshold swing of 0.65 V dec^{-1}, which is critical in low voltage operation. In these results, the potential of non-hydrolytic sol–gel ZrO_2 high-*k* dielectrics for the enhancement of TFT device performance was successfully demonstrated.

Conflicts of interest

There are no conflicts of interest to declare.

Acknowledgements

This work was supported by Samsung Advanced Institute of Technology.

Notes and references

1 A. I. Kingon, J.-P. Maria and S. K. Streiffer, *Nature*, 2000, **406**, 1032.
2 J. Robertson, *Rep. Prog. Phys.*, 2006, **69**, 327.
3 J. Tang, J. Fabbri, R. D. Robinson, Y. Zhu, I. P. Herman, M. L. Steigerwald and L. E. Brus, *Chem. Mater.*, 2004, **16**, 1336.
4 G. D. Wilk, R. M. Wallace and J. M. Anthony, *J. Appl. Phys.*, 2001, **89**, 5243.
5 J.-B. Seon, S. Lee, J. M. Kim and H.-D. Jeong, *Chem. Mater.*, 2009, **21**, 604.
6 S. Acosta, P. Arnal, R. J. P. Corriu, D. Leclercq, P. H. Mutin and A. Vioux, *Mater. Res. Soc. Symp. Proc.*, 1994, **346**, 43.
7 R. J. P. Corriu, D. Leclercq, P. Lefevre, P. H. Mutin and A. Vioux, *J. Non-Cryst. Solids*, 1992, **146**, 301.
8 P. Arnal, R. J. P. Corriu, D. Leclercq, P. H. Mutin and A. Vioux, *Chem. Mater.*, 1997, **9**, 694.
9 M. Andrianainarivelo, R. J. P. Corriu, D. Leclercq, P. Lefevre, P. H. Mutin and A. Vioux, *J. Sol-Gel Sci. Technol.*, 1997, **8**, 89.
10 J. N. Hay and H. M. Raval, *J. Mater. Chem.*, 1998, **8**, 1233.
11 J. N. Hay and H. M. Raval, *J. Sol-Gel Sci. Technol.*, 1998, **13**, 109.
12 J. N. Hay, D. Porter and H. M. Raval, *J. Mater. Chem.*, 2000, **10**, 1811.
13 J. F. Wager, D. A. Keszler, and R. E. Presley, *Transparent Electronics*, Springer, New York, 2008.
14 H. Kim, Y.-J. Kwack, E.-J. Yun and W.-S. Choi, *Sci. Rep.*, 2016, **6**, 33576.
15 H. Tan, G. Liu, A. Liu, B. Shin and F. Shan, *Ceram. Int.*, 2015, **41**, S349.

16 P. Barquinha, L. Pereira, G. Goncalves, R. Martins, D. Kuscer, M. Kosec and E. Fortunato, *J. Electrochem. Soc.*, 2009, **156**, H824.

17 J. Joo, T. Yu, Y. W. Kim, H. M. Park, F. Wu, J. Z. Zhang and T. Hyeon, *J. Am. Chem. Soc.*, 2003, **125**, 6553.

18 C. R. Kagan and P. Andry, *Thin-Film Transistors*, Marcel Dekker, New York, 2003.

19 D. K. Hwang, K. Lee, J. H. Kim and S. Im, *Appl. Phys. Lett.*, 2006, **89**, 093507.

20 S. M Sze and K. K. Ng, *Physics of Semiconductor Devices*, Wiley, Hoboken, 2007.

21 C. D. Dimitrakopoulos, S. Purushothaman, J. Kymissis, A. Callegari and J. M. Shaw, *Science*, 1999, **283**, 822.

22 C. D. Dimitrakopoulos, I. Kymissis, S. Purushothaman, D. A. Neumayer, P. R. Duncombe and R. B. Laibowitz, *Adv. Mater.*, 1999, **11**, 1372.

23 S. Lee, D.-J. Yun, S.-W. Rhee and K. Yong, *J. Mater. Chem.*, 2009, **19**, 6857.

24 P. G. Le Comber and W. E. Spear, *Phys. Rev. Lett.*, 1970, **25**, 509.

25 E. Lee, J. Ko, K.-H. Lim, K. Kim, S. Y. Park, J. M. Myoung and Y. S. Kim, *Adv. Funct. Mater.*, 2014, **24**, 4689.